Thermoplastic Olefin/Clay Nanocomposites: Morphology and Mechanical Properties

Sameer Mehta,[1] Francis M. Mirabella,[1] Karl Rufener,[1] Ayush Bafna[2]

[1]*Equistar Chemicals, LP, 11530 Northlake Drive, Cincinnati, Ohio 45249*
[2]*Department of Chemical and Materials Engineering, University of Cincinnati, Cincinnati, Ohio 45221-0012*

Received 7 March 2003; accepted 17 September 2003

ABSTRACT: Thermoplastic olefin (TPO)/clay nanocomposites were made with clay loadings of 0.6–6.7 wt %. The morphology of these TPO/clay nanocomposites was investigated with atomic force microscopy, transmission electron microscopy (TEM), and X-ray diffraction. The ethylene–propylene rubber (EPR) particle morphology in the TPO underwent progressive particle breakup and decreased in particle size as the clay loading increased from 0.6 to 5.6 wt %. TEM micrographs showed that the clay platelets preferentially segregated to the rubber–particle interface. The breakup of the EPR particles was suspected to be due to the increasing melt viscosity observed as the clay loading increased or to the accompanying chemical modifiers of the clay, acting as interfacial agents and reducing the interfacial tension with a concomitant reduction in the particle size. The flexural modulus of the injection moldings increased monotonically as the clay loading increased. The unnotched (Izod) impact strength was substantially increased or maintained, whereas the notched (Izod) impact strength decreased modestly as the clay loading increased. © 2004 Wiley Periodicals, Inc. J Appl Polym Sci 92: 928–936, 2004

Key words: poly(propylene) (PP); clay; nanocomposites; impact resistance; stiffness

INTRODUCTION

Polypropylene (PP) is one of the most widely used polyolefins, not only because of its balance of physical and mechanical properties but also because of its recycling ability and low cost. However, PP is brittle and has poor low-temperature properties, but the addition of rubber, such as ethylene–propylene rubber (EPR), results in dramatic improvements in these properties. These rubber-modified PPs are often called thermoplastic olefins (TPOs). The rubber toughening of PP continues to be an active area of investigation.[1] It is well known from previous studies that, among other factors, the rubber particle diameter is of critical importance.[1–3] These studies indicate that the modification in the rubber domain size up to an optimum diameter improves the impact strength of PP. It is also well known that the addition of rubber to PP results in a decrease in stiffness.[4] Thus, although successes in improving the impact properties of PP have been attained by rubber toughening, its application (e.g., in the automotive industry) is still limited because of the opposing trends of stiffness and toughness.

The addition of mineral fillers, such as talc and glass, to PP provides an increase in stiffness, but these particulates are stress concentrators and result in a concomitant decrease in the impact strength.[5,6] In recent years, the addition of nanoparticulate fillers such as organically modified clay has been shown to be an effective strategy for achieving improved stiffness in PP.[7–11] The modified clay layers have polar groups on their surfaces and are thus incompatible with nonpolar polymers such as PP. For this reason, most of the studies[12,13] on polyolefin–clay nanocomposites use a functionalized oligomer such as maleic anhydride modified polyolefin as a compatibilizer. The fact that the filler is at the nanometer scale in these systems gives the promise of achieving improved stiffness without a significant loss of impact strength.[14] This is under the assumption that the clay platelets do not act as stress concentrators because of their nanometer scale. Thus, this desirable combination of improved stiffness and maintenance of impact strength through the addition of clay in TPOs, if attained, could boost the applications of TPOs in the automotive industry and other industries. For example, Oldenbo,[15] from Volvo Car Corp. (Sweden), recently presented data regarding the effect of the addition of clay on the impact and flexural properties of TPO/clay nanocomposites. A desirable combination of improvements in the stiffness and maintenance of the impact strength has not been observed in TPO/clay nancomposites.[15] Furthermore, no studies regarding the effect of the addition of clay on the morphology and the relationship between the morphology and property improvement of TPO/clay nanocomposites have been published. Recently, claims in the patent literature[16] and

Correspondence to: F. M. Mirabella (francis.mirabella@equistarchem.com).

Journal of Applied Polymer Science, Vol. 92, 928–936 (2004)

TABLE I
Composition and Properties of TPO/Clay Nanocomposites

Sample	Clay loading (wt %)	Compatibilizer (wt %)	Flexural modulus (kpsi)	Izod unnotched impact strength at −18°C (ft-lb/in.)	Izod notched impact strength at −18°C (ft-lb/in.)
TPO-0	0	0	103.5	22.4	8.1
TPO-1	0.6	0.25	119.1	30.0	11.7
TPO-2	1.2	0.5	115.7	33.2	10.9
TPO-3	2.3	1.0	121.9	27.9	9.3
TPO-4	3.3	1.5	130.9	33.1	7.6
TPO-5	4.4	2.0	135.6	35.1	3.1
TPO-6	5.6	2.5	141.4	33.7	6.4
TPO-7	6.7	3.0	153.1	22.4	6.0

in a trade journal[17] have been made concerning TPO/clay nanocomposites.

In this study, the effect of varying the clay loading (0.6–6.7 wt %) on the morphology of TPO/clay nanocomposites was studied with atomic force microscopy (AFM), transmission electron microscopy (TEM), and X-ray diffraction (XRD). This article, the only one of its kind of which we are aware, examines the morphological and mechanical property data of TPO/clay nanocomposites. The clay morphology and the relationship between the presence of clay and the dispersed-phase morphology of the TPO are discussed. These observed morphologies are compared to the mechanical behavior of the nanocomposites at various clay loadings.

EXPERIMENTAL

Materials

A commercial TPO was used with a 9.5 melt-flow rate (MFR) and a 103,500 psi flexural modulus. The TPO was composed of about 70 wt % isotactic PP and about 30 wt % EPR. The nanocomposites (see Table I) were prepared through the blending of the TPO with maleic anhydride grafted polypropylene (PP-MA; 1.0% maleic anhydride) as a compatibilizer and with a natural montmorillonite clay modified with a quaternary ammonium salt (Cloisite 20A, Southern Clay Products, Gonzales, TX).

Processing

The TPO (25%), PP-MA (25%), and clay (50%) were initially compounded and pelletized into a master batch with a ZSK 30 twin-screw extruder (Coperion Corp., Ramsey, NJ). This master batch was compounded in different proportions with the TPO to vary the clay loading in the nanocomposite. The pellets were then injection-molded with a Battenfeld injection-molding machine (West Warwick, RI) into test specimens for impact and flexural testing.

Microscopy and stereology

We prepared cross sections for TEM by first facing the nanocomposite off with a diamond knife in a cryo ultramicrotome, then staining it with ruthenium tetroxide for 8 h, and finally cross-sectioning it into 40-nm-thick sections with a Reichert–Jung FC4E cryo ultramicrotome (Mager Scientific, Inc., Dexter, MI). TEM observations were made with a JEOL EM-ASI D10 TEM (Peabody, MA) with an acceleration voltage of 120 kV. AFM was performed on cryogenically microtomed surfaces with a Digital Instruments Nanoscope IIIA with a Phase and Dimension 3100 atomic force microscope (Veeco Metrology LLC, Santa Barbara, CA). The three-dimensional particle number-average diameters were deduced from the two-dimensional AFM images by well-known methods described previously.[18]

XRD

XRD was performed for the organophilic clay (Cloisite 20A), TPO control, and TPO nanocomposites with a Phillips diffractometer (PANalytical, Natick, MA), which had a graphite monochromator and a Cu Kα radiation source and was operated at 40 kV and 30 mA. The camera operated in reflection geometry. The samples were scanned at a scanning speed of 1°/min in the 2θ range of 2.5–10°.

MFR

MFR was measured according to ASTM D 1238.

Rheology

Rheological measurements were made in the frequency range of 0.1–400 rad/s at 210°C on an ARES rheometer manufactured by Rheometric Scientific (Piscataway, NJ).

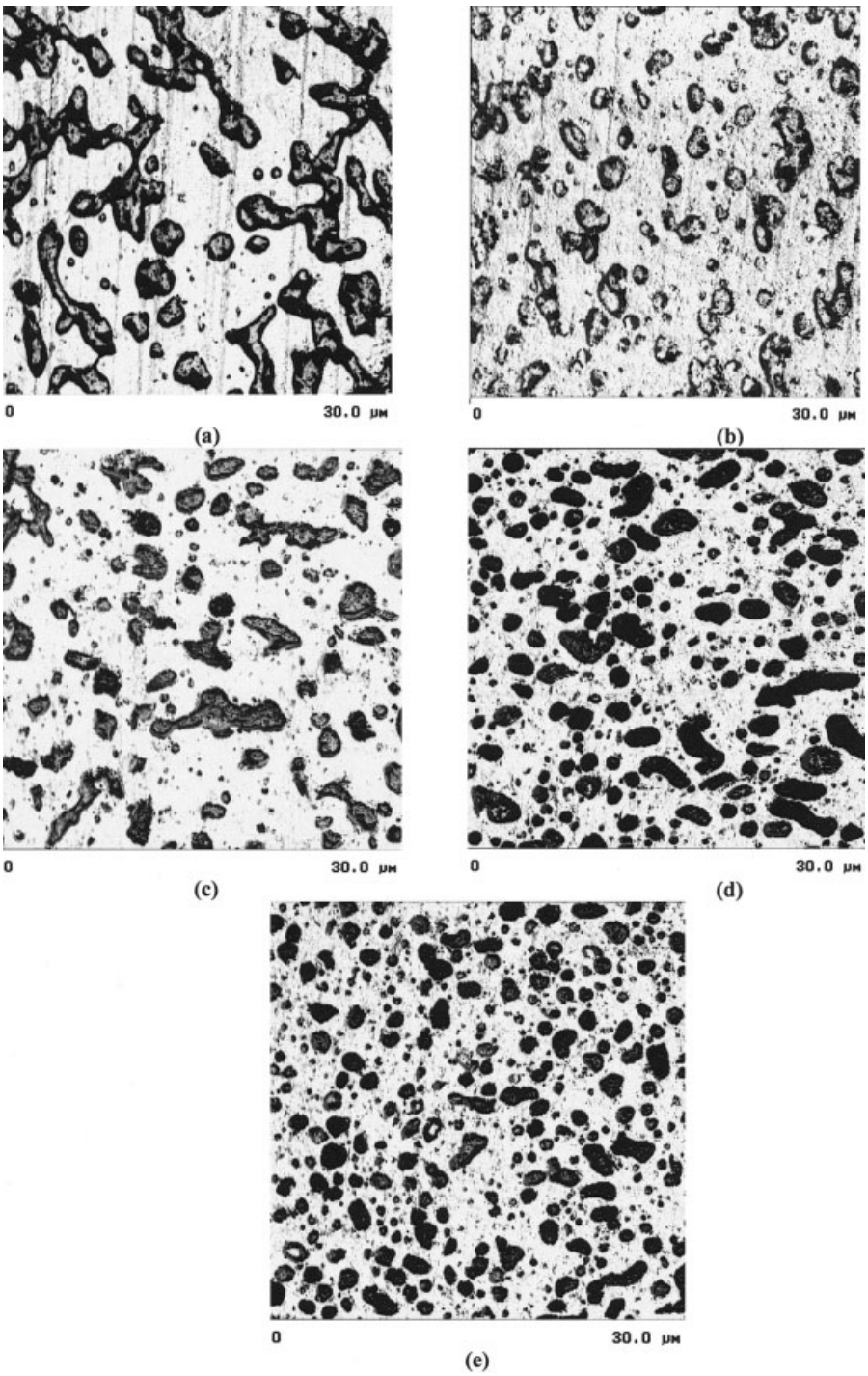

Figure 1 AFM phase images of (a) TPO-0 (0 wt % clay), (b) TPO-1 (0.6 wt % clay), (c) TPO-3 (2.3 wt % clay), (d) TPO-4 (3.3 wt % clay), and (e) TPO-6 (5.6 wt % clay).

Mechanical testing

The flexural modulus was the 1% secant modulus measured according to ASTM D 790B. The error associated with the flexural modulus test was ±5% (relative). The unnotched Izod at −18°C was measured according to ASTM D 4812. The error associated with the unnotched Izod test was ±25% (relative). The notched Izod at −18°C was measured according to ASTM D 256. The error associated with the notched Izod test was ±25% (relative).

RESULTS AND DISCUSSION

The morphology of the unmodified (control) TPO and TPO/0.6 wt % clay, TPO/2.3 wt % clay, TPO/

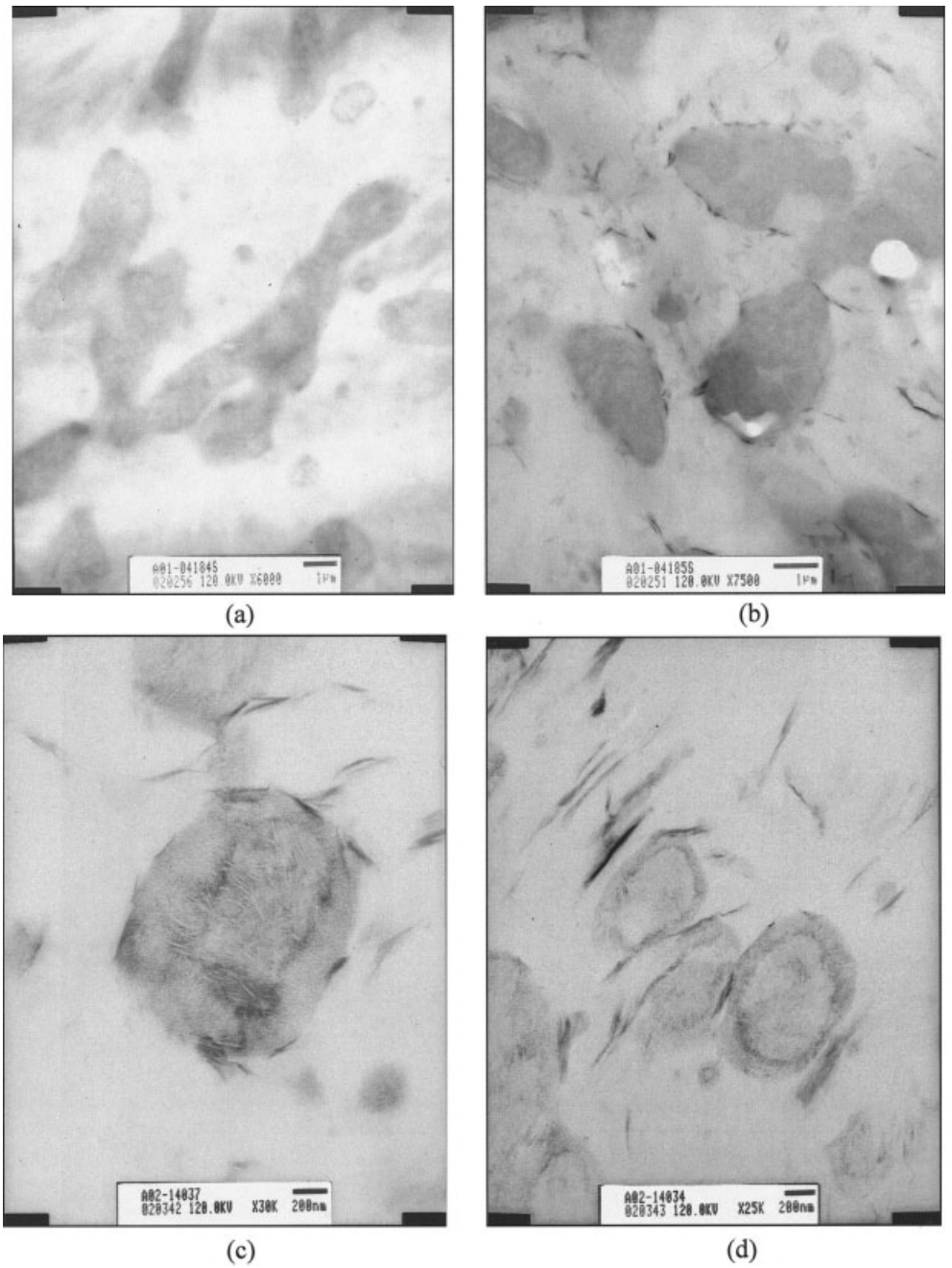

Figure 2 TEM micrographs (at various magnifications) of (a) TPO-0 (0 wt % clay), (b) TPO-1 (0.6 wt % clay), (c) TPO-3 (2.3 wt % clay), and (d) TPO-6 (5.6 wt % clay). Rubbery domains (elliptically shaped) surrounded by clay platelets (dark, rodlike structures) can clearly be seen.

3.3 wt % clay, and TPO/5.6 wt % clay nanocomposites are compared with AFM images in Figure 1(a–e), respectively. The EPR particles exhibit a reduction in the average particle diameter as the clay loading increases. Figure 1(a–e) shows that the EPR particles in the unmodified TPO coalesce together into multiparticle clusters, which are broken up into smaller single particles, as the clay loading increases.

As can be observed in the TEM images in Figure 2(a–d), these TPO/clay systems largely exhibit a dispersion of the clay into stacks about 10–50 nm thick, corresponding to stacks of about 5–25 clay platelets. These stacks are often called *tactoids* and exhibit a clay spacing (clay long period) of about 2–3 nm, as measured by XRD (the unmodified clay spacing was ca. 1 nm). The XRD patterns for the modified clay, TPO control, and nanocomposites are shown in Figure 3. The mean clay spacing of the (001) planes for the clay layers in the nanocomposites is 2.2 nm ($2\theta = 4°$). The intensity of the scattered X-rays depends on the loading of the clay in the nanocomposite. Thus, the inten-

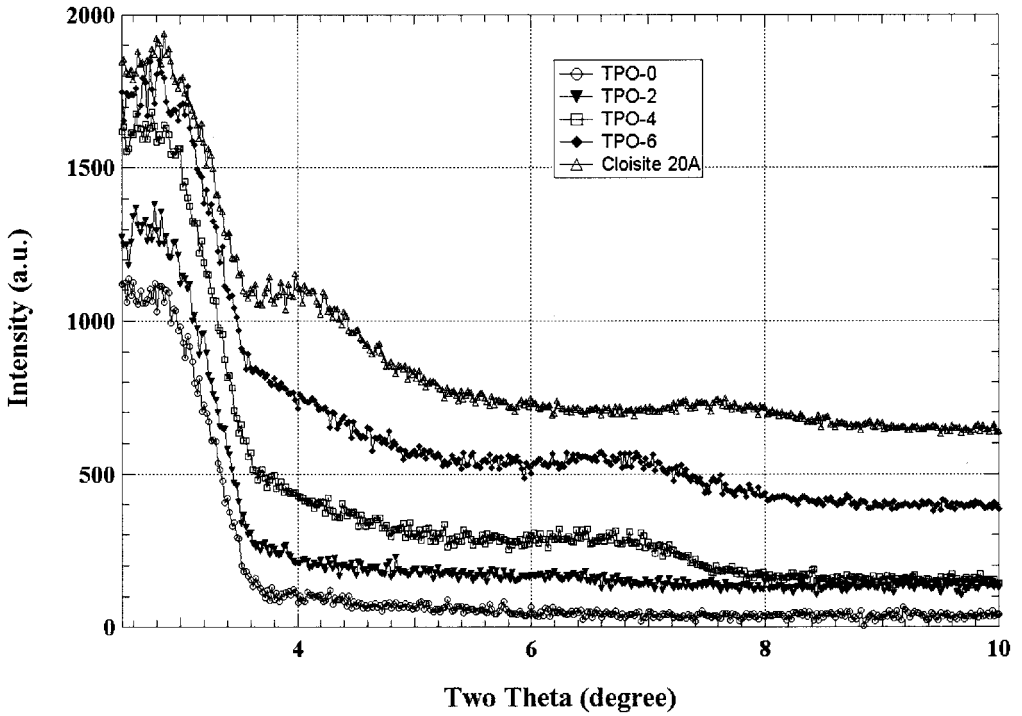

Figure 3 XRD patterns of unmodified TPO, organophilic clay (Cloisite 20A), and TPO/clay nanocomposites. The diffraction patterns were arbitrarily shifted along the *y* axis to facilitate viewing.

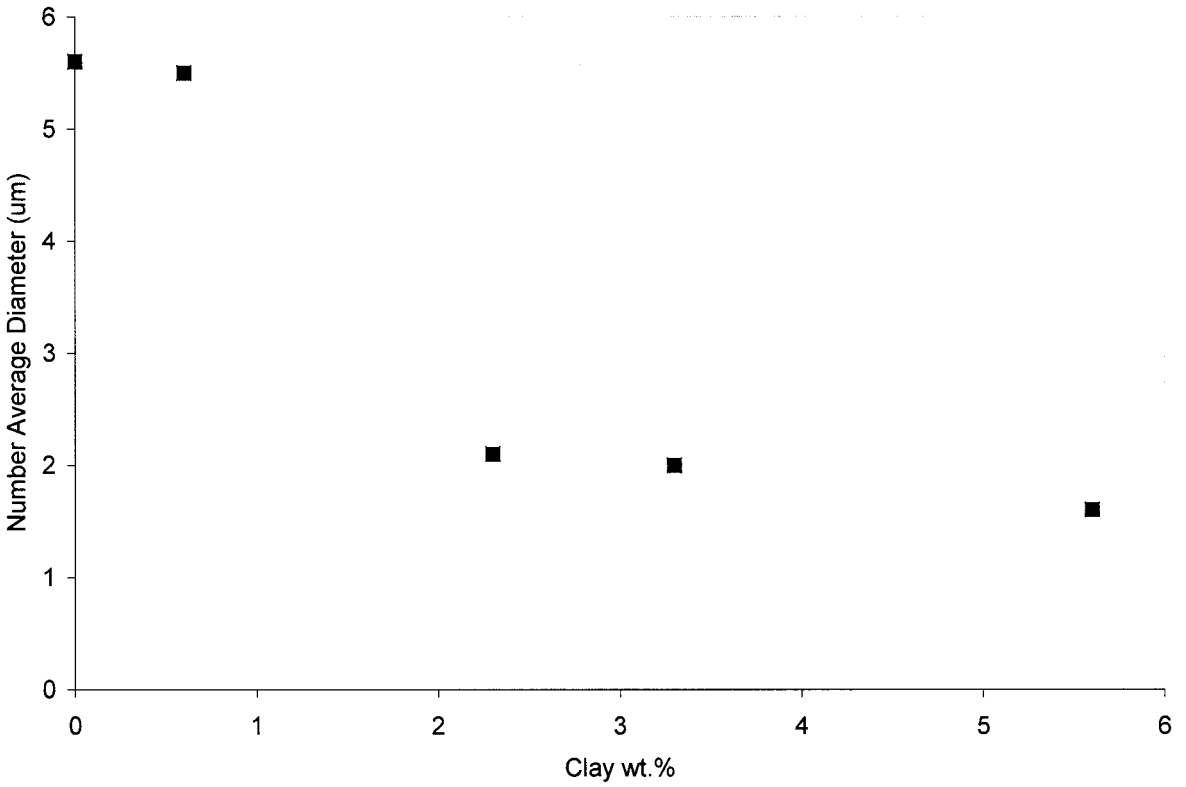

Figure 4 Number-average particle diameter of EPR versus the weight percentage of clay in TPO.

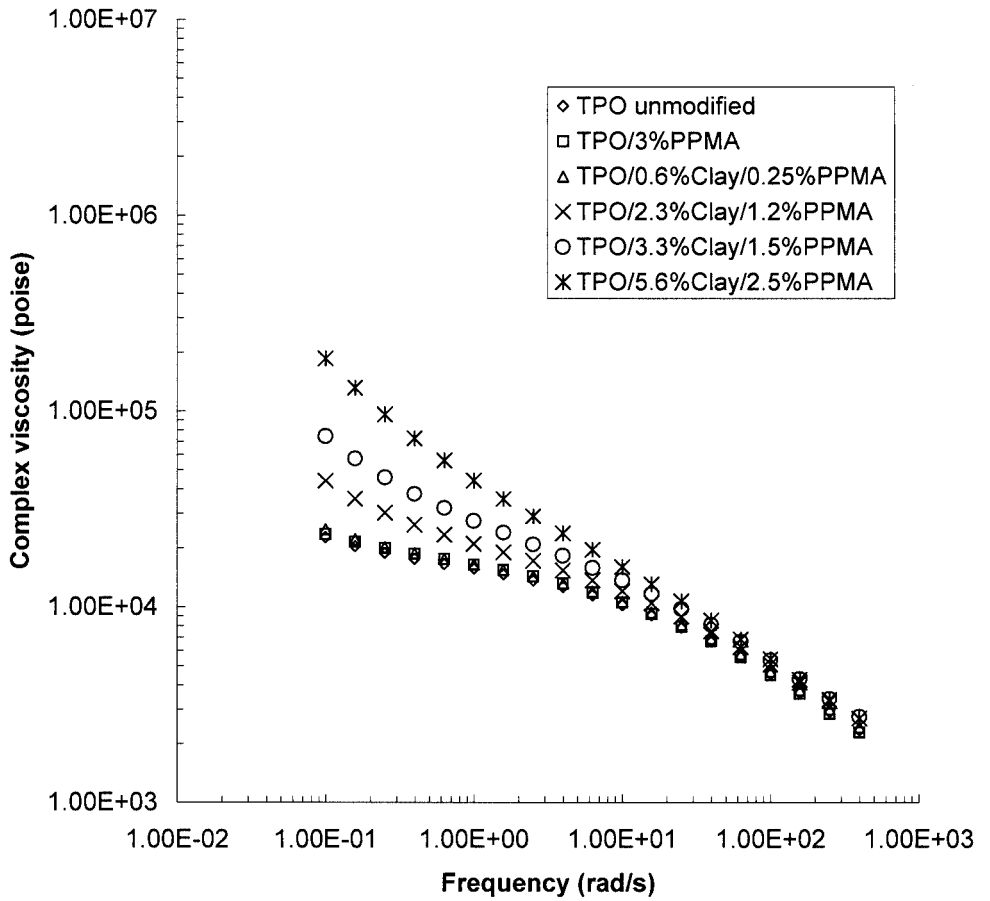

Figure 5 Rheological data for unmodified TPO, TPO/PP-MA, and TPO/PMMA/clay nanocomposites.

sity of the clay peak at $2\theta = 4°$ decreases as the clay loading decreases. For this reason, no or very little scattering was observed in samples TPO-0 and TPO-1, respectively. The tactoids represent the modified clay (i.e., containing the quaternary ammonium salt modifier) and compatibilizer (i.e., PP-MA with 1.0% maleic anhydride) in the polymer. Figure 2(a–d) also shows that more highly dispersed clay is evident in which fewer clay platelets are stacked together. Furthermore, Figure 2 shows that the clay platelets are largely preferentially segregated to the EPR/matrix interface and dispersed in the matrix. Because the clay is not truly exfoliated into individual clay platelets, the measurement of the clay spacing in any of these systems by XRD consistently has shown a clay spacing of 2.2 nm, which is the spacing in the tactoids observed by TEM. Therefore, the XRD measurements are of little value in characterizing the clay dispersion.

The change in the EPR number-average particle diameter with the clay loading is shown in Figure 4. The particle diameter decreases by a factor of about 3 as the clay loading increases from 0 to 5.6 wt %.

The effects of the compatibilizer and the clay addition to the TPO rheology are shown in Figure 5. The compatibilizer alone has no effect on the viscosity–frequency curve, with respect to the unmodified TPO. However, systems with increasing clay loading exhibit strongly increasing viscosity. The increase in the melt viscosity of PP/clay nanocomposites is well known. Galgali et al.[19] showed that the zero shear viscosity increased in PP/clay nanocomposites without a compatibilizer, and it increased more dramatically in systems with a compatibilizer.

The systematic modification of the dispersed, rubber-phase morphology, shown in Figure 1, may be due to one or both of the following mechanisms. The increasing viscosity with clay loading, as observed in the rheological measurements, may be contributing to this effect. The melt viscosity ratio of the EPR dispersed phase to the PP matrix (p = EPR viscosity/polypropylene viscosity) is known to control the rubber particle coalescence and breakup during shearing.[20] Typically, as this ratio approaches 1, the particle size decreases and reaches a minimum value at $p = 1$. This ratio is apparently changing, as indicated by the changing system rheology shown in Figure 5. Alternatively, the clay platelets, the accompanying chemical modifiers of the clay, and the compatibilizer may act as interfacial agents, reducing the interfacial ten-

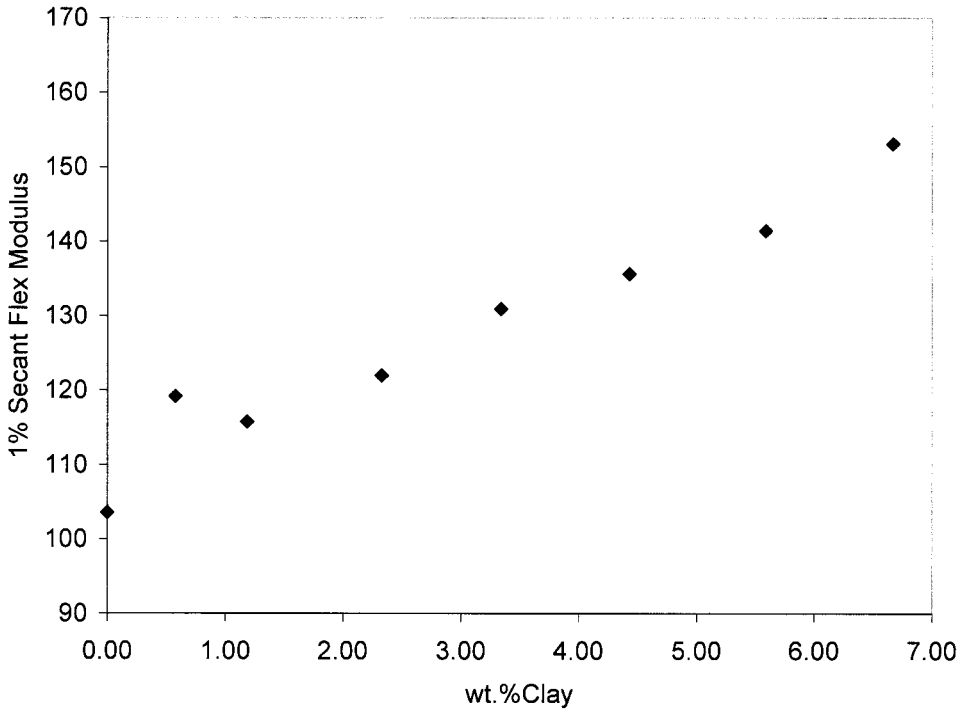

Figure 6 TPO/clay flexural modulus versus the clay content.

sion with a concomitant breakup of the EPR particles and a reduction in the particle size.

The mechanical properties also undergo modification. Figure 6 shows a monotonic increase in the flexural modulus as the clay loading increases. The flexural modulus increases by about 50% as the clay loading increases from 0 to 6.7 wt %. The increase in the flexural modulus is well outside the standard deviation of this test, which is ±5% (relative). The dramatic increase in the flexural modulus in the case of these

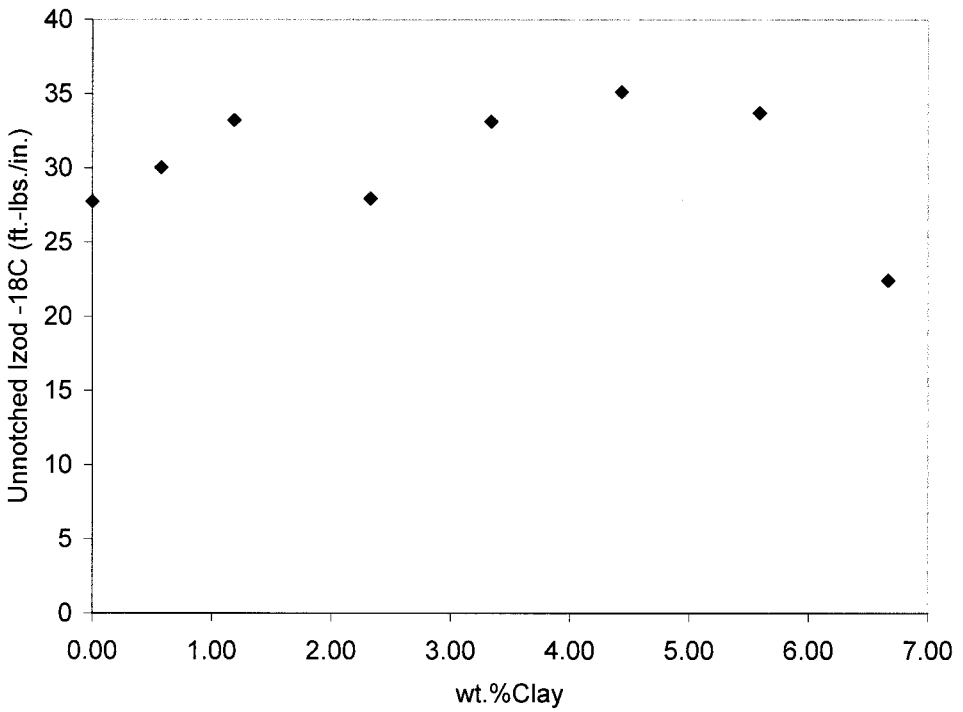

Figure 7 TPO/clay unnotched Izod impact strength versus the clay content.

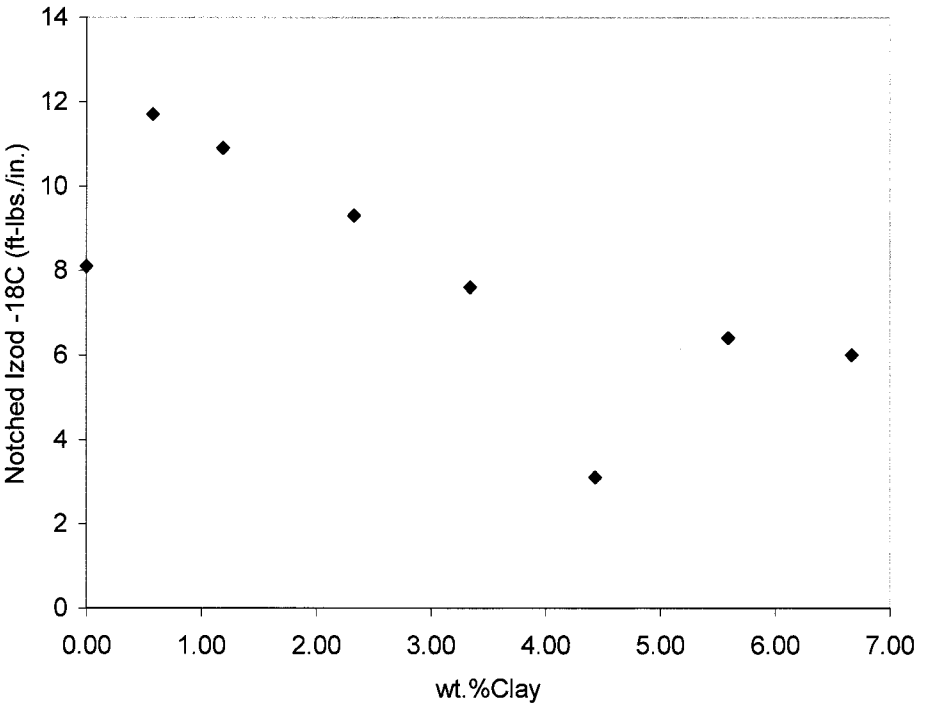

Figure 8 TPO/clay notched Izod impact strength versus the clay content.

TPO/clay systems, in which intercalation, not exfoliation, of the clay layers is observed, is consistent with other studies.[15] The cause for the dramatic increase in stiffness is suspected to be due to anisotropic orientation of the clay platelets in the injection moldings, as observed in other studies.[15] The increase in the flexural modulus is similar to that observed for microdispersed inorganic fillers, such as talc at about a 5 times higher loading of talc.[15] Figure 7 shows that the impact strength, as measured by the unnotched Izod at −18°C, substantially increases or remains nearly constant as the clay loading increases. Considering that the standard deviation of this test is quite large at ±25% (relative), it must be noted that some of the variation observed in the unnotched Izod is within the error limits of the test. Therefore, the apparent substantial increase in the unnotched Izod may be partially explained by error fluctuations in the data. Figure 8 shows that the impact strength, as measured by the notched Izod at −18°C, exhibits an initial increase followed by a steady, but modest, decrease as the clay loading increases. Considering that the standard deviation of this test is quite large at ±25% (relative), it must be noted that some of the variations observed in the notched Izod are within the error limits of the test. Therefore, the apparent initial increase and subsequent decrease in the notched Izod may be partially explained by error fluctuations in the data. It must be concluded that the notched Izod decreases steadily and modestly as the clay loading increases from 0 to 6.7 wt %. At the highest clay loadings, a trend of sharply decreasing impact strength has been noted, indicating that clay loadings higher than 6.7 wt % are expected to exhibit further reductions in the impact strength.

CONCLUSIONS

The EPR morphology in TPO/clay nanocomposites undergoes progressive particle breakup and a reduction in the particle size as the clay loading increases from 0.6 to 5.6% clay. This has been ascribed to two potential mechanisms: (1) the melt viscosity increases as the clay loading increases, and this may play a role in the control of the particle size through shear-mixing coalescence and breakup, and (2) the clay preferentially segregates to the rubber particle/matrix interface, and it is suspected that the progressive breakup of the EPR particles is due to the action of the clay, associated chemical modifiers, and the compatibilizer on the clay as interfacial agents. The flexural modulus of injection moldings increases by about 50% as the clay loading increases from 0.6 to 6.7 wt %. The unnotched (Izod) impact strength substantially increases or remains steady, whereas the notched (Izod) impact strength decreases modestly, as the clay loading increases from 0.6 to 6.7 wt %.

References

1. Jang, B. Z.; Uhlmann, D. R.; Vander Sande, J. B. J Appl Polym Sci 1985, 30, 2485.

2. Jang, B. Z.; Uhlmann, D. R.; Vander Sande, J. B. In Proc 42nd Annu Tech Conf, New Orleans, LA, 1984, vol. 30, p 549.
3. Mehrabzadeh, M.; Hossein Nia, K. J Appl Polym Sci 1999, 72, 1257.
4. Lu, J.; Wei, G.-X.; Sue, H.-J.; Chu, J. J Appl Polym Sci 2000, 76, 311.
5. Radosta, J. A. In Proc 42nd Annu Tech Conf, New Orleans, LA, 1984, vol. 30, p 145.
6. Marshall, C. J.; Rozett, R.; Kunkle, A. C. Plast Compd 1985, Nov/Dec, 69.
7. Oya, A.; Kurokawa, Y. J Mater Sci 2000, 35, 1045.
8. Kodgire, P.; Kalgaonkar, R.; Hambir, S.; Bulakh, N.; Jog, J. J Appl Polym Sci 2001, 81, 1786.
9. Svoboda, P.; Zeng, C.; Wang, H.; James Lee, L.; Tomasko, D. J Appl Polym Sci 2002, 85, 1562.
10. Hasegawa, N.; Okamoto, H.; Kato, M.; Usuki, A. J Appl Polym Sci 2000, 78, 1918.
11. Hasegawa, N.; Kawasumi, M.; Kato, M.; Usuki, A.; Okada, A. J Appl Polym Sci 1998, 67, 87.
12. Wang, K. H.; Choi, M. H.; Koo, C. M.; Choi, Y. S.; Chung, I. J. Polymer 2001, 42, 9819.
13. Kodgire, P.; Kalgaonkar, R.; Hambir, S.; Jog, J. J Appl Polym Sci 2001, 81, 1786.
14. Svoboda, P.; Zeng, C.; Wang, H.; Lee, L. In Proceedings of Nanocomposites 2001, Chicago, IL, 2001.
15. Oldenbo, M. In Proceedings of Nanocomposites 2001, Chicago, IL, 2001.
16. Niyogi, S. G. U.S. Pat. 6,451,897 (2002).
17. Mod Plast 2000, 77, 72.
18. Mirabella, F. M. J Polym Sci Part B: Polym Phys 1994, 32, 1205.
19. Galgali, G.; Ramesh, C.; Lele, A. Macromolecules 2001, 34, 852.
20. Wu, S. Polym Eng Sci 1987, 27, 335.